The HEXV-15 Kestrel

Executive Summary

Undergraduate Team
Delft University of Technology

Boutros, M.A. ⋄ Van Duuren, R.J. ⋄ Gruters, E.A. ⋄ Limnidis, P. ⋄ Nair, R. ⋄ Polak, M.T.

Main Supervisor: Prof. Dr. M.D. Pavel. Secondary Supervisors: I. Komala, A.S. Correira.

Vertical Flight Society
43rd Annual Student Design Competition
June 2026

Executive Summary

Advanced Air Mobility (AAM) is motivated by a practical need rather than novelty: to enable fast, flexible regional transport from space-constrained infrastructure whilst meeting increasingly stringent regulations on safety, noise, and emissions. Vertical Take-Off and Landing (VTOL) aircraft are a natural fit for this operating concept. Conventional rotorcraft, however, are typically limited by cruise efficiency and noise, while hybrid-electric VTOL concepts additionally remain constrained by energy density at the scale required for medium-range operations. Tiltrotors offer an established compromise by combining VTOL capabilities with fixed-wing cruise efficiency , despite being challenged by high acoustic noise, cost, emissions and operational complexity.

The Hybrid-Electric XV-15 Kestrel (HEXV-15) is developed from this position. It uses the Bell XV-15 as a traceable tiltrotor baseline and investigates whether a legacy tiltrotor can be transformed into a hybrid-electric regional AAM aircraft without losing the payload-range capability that makes the configuration operationally relevant. The intent is to develop a near-term and certifiable vehicle that is particularly well-suited for regional VTOL operations, whilst minimising its emissions and development costs. To achieve these goals, the final aircraft cannot be a battery installation exercise. Instead, it has to be a coupled redesign in which hybrid-electric propulsion, proprotor efficiency, wing aerodynamic efficiency, structural mass recovery, thermal management, control margins, and operational energy management are treated as one system-level problem.

The resulting HEXV-15 concept (Phase II) is shown in Figure 1, where the novelty of the design can readily be observed in the nacelle-mounted wing extensions. A closer look at the vehicle would reveal fully updated proprotor and wing designs, an overhaul of the aircraft structures, modular energy storage, and integration of hybrid-electric architecture; all with the goal of limiting the vehicle's emissions whilst maximising its payload-range capabilities. This establishes the HEXV-15 as an evolution of the Bell XV-15, with a much smaller development budget than any clean-sheet configuration.

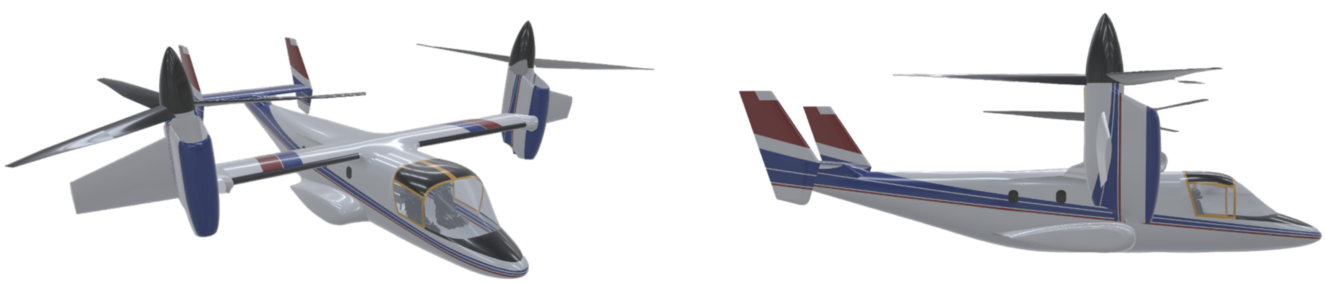

Figure 1: HEXV-15 Kestrel hybrid-electric tiltrotor concept (Phase II). The aircraft retains the XV-15 tiltrotor architecture, cross-shafted drivetrain philosophy, and three-bladed proprotors, while introducing nacelle-mounted wing extensions, optimised proprotor geometry, modular battery storage, and a high-voltage hybrid-electric torque-assist system.

Central Result

The Phase II HEXV-15 Kestrel closes the Request For Proposal (RFP) reference mission with 726 kg (1600 lb) payload, 18% energy-based Degree of Hybridisation (DoH), 1303 kg (2873 lb) of battery mass, 415 kg (915 lb) of fuel, and a reported VTOL MTOM of 6804 kg (15,000 lb). This is the design point for the RFP reference mission, repeated in Figure 2. The inclusion of battery modularity results in a maximum range of 1016 km (631 mi) at 17% hybridisation, and 271 km (168 mi) with 58% hybridisation for the same payload mass when the hover phases are omitted from the RMP. With an estimated project development cost of 50 M EUR (59 M USD), the design can be realised within four years.

The programme design objectives in Table 1 form the common basis for the development of the HEXV-15 Kestrel. In addition, they serve as the criteria for all system- and subsystem-level trade-offs performed in the design, which follow the Multiple-Critera Design Analysis (MCDA) methodology detailed in the NASA Systems Engineering handbook . Employment of these design objectives, or objectives derived from this set but made suitable for a particular subsystem, ensures that all (re)designed subsystems are developed with a common rationale.

Table 1: Programme-level design objectives used as the basis for the vehicle development and for all system and subsystem trade-off criteria, derived from Leonardo's RFP .

Objective	Design objective description
PRG-01	Minimise HEXV-15 development and production cost.
PRG-02	Minimise HEXV-15 Empty Mass (EM).
PRG-03	Minimise HEXV-15 environmental impact.
PRG-04	Maximise HEXV-15 mission range capabilities.
PRG-05	Maximise HEXV-15 vehicle and operational reliability.
PRG-06	Maximise usage of existing Bell XV-15 componentry in the HEXV-15.

Reference Mission and Certification Framing

The design is sized against a single Reference Mission Profile (RMP), as shown in Figure 2, which is an expanded version of the RFP mission and is defined dispatch-to-dispatch. The RMP is used to avoid inconsistent conclusions between propulsion size, payload-range capability, emissions, noise, and cost. It covers the mandated climb, cruise, descent and landing procedures, but it also features vertiport operations . Inclusion of requirements from this conceptual EASA certification standard ensures readiness for future urban operations, negating a future need for redesigns to match certification needs. It additionally provides a more realistic basis for noise emission calculations, operational concept developments and especially turnaround-relevant handling of the new hybrid-electric architecture.

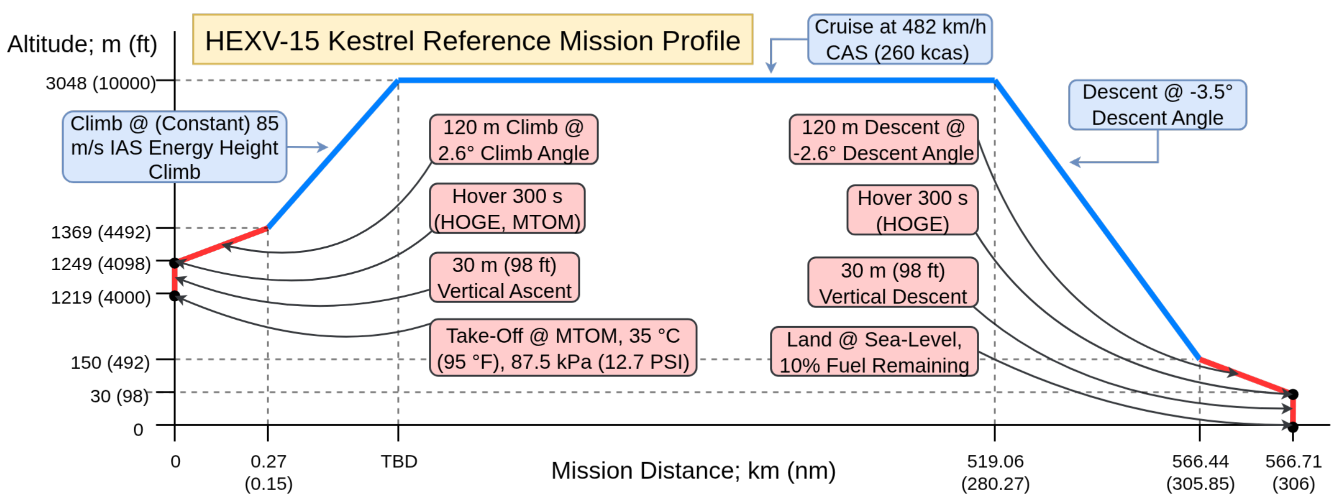

Figure 2: Reference Mission Profile used for sizing and assessment of the HEXV-15. The required useful cabin payload is 726 kg (1600 lb), corresponding to six passengers in addition to two pilots of 100 kg (220 lbs) each. International Standard Atmosphere conditions are assumed unless stated otherwise. The horizontal distance covered during the climb to cruise is left as TBD, as it depends on the excess power of the vehicle in this phase. Note that the axes are not to scale.

The certification basis of the Kestrel is treated as an inherent design driver throughout its development. Since the vehicle combines rotor-borne flight, wing-borne flight, conversion, and hybrid-electric propulsion, a single conventional certification code cannot capture the complete design. The aircraft is therefore framed against a combined EASA certification basis, justified by the applicability specified in their documentation. CS-29 is used as the primary rotorcraft reference , CS-23 supports wing-borne operation , and special-condition logic is applied to the powered-lift and electric/hybrid propulsion elements. SC-VTOL is relevant for transition and VTOL operational safety, while SC-E-19 is relevant for electric and hybrid propulsion integration, high-voltage distribution, battery safety, functional safety, and thermal management . The resulting preliminary certification basis led to a large amount of design requirements. The main roles of each certification types are summarised in Table 2.

Table 2: Combined EASA certification framing for the HEXV-15, used as a preliminary design driver.

Basis	Role in design	Resulting design consequence
CS-29	Primary basis for vertical flight, rotorcraft load and OEI logic, hover, and powered take-off/landing behaviour.	Requires the hybrid-electric architecture to remain compatible with safe continued flight and landing following critical failures.
CS-23	Wing-borne flight, V-n envelope, gust loads, and aeroplane-mode performance.	Drives the wing extension, manoeuvre/gust envelope, structural factor of safety, and speed-margin checks.
SC-VTOL	Transition, conversion, and VTOL-specific safety objectives.	Requires explicit consideration of conversion corridor, degraded operation, and safety of the tiltrotor transition regime.
SC-E-19	Electric and hybrid propulsion, high-voltage safety, battery and TMS integration.	Drives the 950 VDC architecture, battery management, cooling, modular replacement concept, and failure containment assumptions.

This framing directly affects the technical design strategy. Given the complexity of the certification basis, maximising novelty across every subsystem would press technology readiness and prolong certification; high-TRL XV-15 elements are therefore retained, including the cross-shafted drivetrain, three-bladed proprotors and turboshaft backbone. Novelty is instead concentrated where it produces quantifiable mission benefits at lower risk: modular battery packs, nacelle-mounted wing extensions, optimised proprotor geometry, high-voltage torque assist, and RPM/noise scheduling.

RFP Requirement Compliance and Design Traceability

To kickstart the technical development of the HEXV-15, an ECSS-style translation was performed of the RFP constraints, Reference Mission Profile, stakeholder and market analyses and preliminary certification framing, leading to an extensive set of mission, stakeholder, system, and subsystem requirements. These requirements complement the programme-level design objectives and provide the technical traceability between the competition task, the operational concept, and the final HEXV-15 configuration. Because the complete requirement set is too extensive for this report, Table 3 retains only the requirements and constraints most relevant to the VFS evaluation, together with the final compliance status.

Table 3: Driving requirements and constraints for the HEXV-15 VFS submission , including compliance for the final Phase II configuration. Note that 'C' stands for 'Compliant' and 'NC' for 'Non Compliant'. Compliance is deemed *preliminary*, as formal confirmation requires analyses of the detailed design or experiments.

Req. ID	Driving requirement / constraint	Status	Justification
MIS-0101	HEXV-15 shall be capable of executing the Reference Mission Profile, as defined in Figure 2.1, whilst under the loading conditions defined by requirements MIS-0201, MIS-0301, MIS-0302 and MIS-0401.	**C**	Final design closes the RMP with 2 pilots of 100 kg (220.5 lbs) each and with 726 kg (1600 lbs) payload on-board, consisting of 6 passengers with luggage.
MIS-0201	HEXV-15 shall be capable of hosting a payload mass of no less than 726 kg (1600 lbs).	**C**	Design point uses 726 kg (1600 lb) RMP payload.
MIS-0301	HEXV-15 shall be crewed by 2 pilots throughout nominal operation.	**C**	Cabin/operations concept retains a two-pilot crew.
MIS-0302	HEXV-15 shall be capable of hosting pilots with a mass of no less than 100 kg (220.5 lbs).	**C**	Crew mass assumption retained as a separate mass contribution in vehicle sizing.
MIS-0401	HEXV-15 shall feature the cabin volume and capabilities to accommodate 6 passengers in addition to the crew for the execution of the Reference Mission Profile.	**C**	Six-passenger payload is retained within the XV-15 cabin concept.
STK-0102	HEXV-15 shall employ hybrid-electric variants of the original Lycoming T53 engines, or of downscaled derivates thereof with specific fuel consumption and rating structure identical to the original.	**C**	Phase II retains the original T53-class turboshaft, without downscaling to provide a power margin for the new VTOL Maximum Take-Off Mass (MTOM). Downscaling still possible.
STK-0103	All batteries on board of the HEXV-15 shall have an energy density of 250 Wh/kg (113 Wh/lb), a power density of 2500 W/kg (1.52 hp/lb) and a volumetric energy density of 600 Wh/L (16,990 Wh/ft$^3)onpacklevel.$	**C**	Battery sizing uses the RFP pack-level energy, power, and volumetric assumptions.
SYS-0110	HEXV-15 shall have a true Maximum Airspeed (V_{NO}, TAS) of no less than 555.6 km/h (300 ktas) at 4572 m (15,000 ft) altitude in standard ISA conditions.	**TBD**	Aeroplane-mode envelope and power curve Figure 16 support an altitude of 9000 m (29,528 ft) at this speed; final confirmation awaits structural assessment.

Continued on next page

Req. ID	Driving requirement / constraint	Status	Justification
SYS-0111	HEXV-15 shall have a true Never Exceed airspeed (V_{NE}, TAS) of no less than 648.2 km/h (350 ktas) at 4572 m (15,000 ft) altitude in standard ISA conditions.	**TBD**	Aeroplane-mode envelope and power curve Figure 16 support an altitude of 8000 m (26,247 ft) at this speed; final confirmation awaits rotor behavioural simulations in these conditions.
SYS-0207	HEXV-15 shall have a Hover Out of Ground Effect (HOGE) capability of no less than 4536 kg (10000 lbs) at an ambient temperature of 35 °C (95 °F) and an ambient pressure of 87.5 kPa (12.7 PSI).	**C**	Final HOGE ceiling is 3014 m (9888 ft) at an MTOM of 6804 kg (15,000 lbs) and ISA conditions.
SYS-0401	HEXV-15 shall feature a structural factor of safety of no less than 1.5 on the limit loads for all its structural elements, unless otherwise specified in lower-level requirements.	**C**	Preliminary structural sizing and wingbox checks use the required safety factor.
SYS-0705	HEXV-15 shall feature autorotation of its rotors in a manner ensuring continued safe flight and landing in case of any sudden loss of thrust at any moment during the execution of the Reference Mission Profile.	**TBD**	Cross-shafted rotorcraft backbone is retained; full autorotation/failure-case demonstration remains certification-stage work.
SYS-0904	HEXV-15 shall feature battery swapping capabilities for all batteries used for nominal operation, ensuring an electrical energy replenishment time of no more than 20 minutes in vertiport operations.	**TBD**	Modular pack replacement is the selected ground concept, in packs carriable by ground crew. Exact replenishment time awaits ground facility design.
SYS-1002	HEXV-15 shall have no less than 10% of its propulsive energy required for completion of the Reference Mission Profile originating from electrical sources, and/or shall distribute it electrically.	**C**	Final design point uses 18% energy-based DoH and high-voltage electrical distribution.
SYS-1201	HEXV-15 shall have a maximum total rotor span (tip-to-tip) of no more than 17.4 m (57.2 ft), equal to the Bell XV-15's maximum rotor span.	**C**	Final HEXV-15 tip-to-tip span equals 17.32 m (56.83 ft).
SYS-PTR-0107	Each proprotor shall have a blade diameter of no more than 7.62 m (25 ft).	**C**	Final diameter is 7.48 m (24.5 ft).
SYS-PTR-0102	Each proprotor shall feature three rotor blades.	**C**	Three-bladed proprotor architecture retained.
SYS-WNG-0306	The HEXV-15 shall have a total wingspan identical to the Bell XV-15's wingspan, being 9.80 m (36.2 ft) [1].	**NC**	Deliberately waived in favour of SYS-1201; final span is 14.42 m (47.3 ft), featuring wing extensions that do not protrude beyond the rotors.

The RFP imposes a two-phase structure, where Phase I preserves the historical XV-15 physical configuration as far as possible: same rotor, wing size, blade aerodynamic properties, maximum design gross weight, and empty weight except for systems directly affected by hybridisation. The performance of all designs present in the report, including the Phase I design, is estimated with an internally developed Hybrid-Electric Mass and Range Solver. This tool integrates the mission shaft-energy demand over the RMP, propagates it through the propulsion-chain efficiencies, splits the required energy between fuel and batteries according to the selected Degree of Hybridisation (DoH). The RMP cruise range is an input to the energy equation as well as the final output. The Hybrid-Electric Mass and Range Solver approaches this problem iteratively, by selecting an initial RMP cruise range and altering the length until the fuel and battery masses close the available mass budget.

This made the central limitation quantitative: direct hybridisation under the original XV-15 VTOL mass constraint and performance collapses the useful payload-range capabilities. Consequently, the Phase I architecture selection is retained as a diagnostic and conceptual baseline, but its propulsive and energy storage sizing is *not* imposed on the Phase II design, in order to maximise the optimisation possibilities. The Phase II design does follow all other RFP requirements on payload, maximum rotor diameter, blade number and so on. This decision allows for the vehicle to be optimised in an integrated manner, where subsystem-level optimisations and designs can be linked together to maximise the feasible hybridisation for the required payload and mission range. This effectively creates an optimisation loop, where the final energy storage sizing is iterated to solve for the maximum energy DoH for the RMP, whilst using the performance of the new hybrid-electric architecture and the optimised subsystems, instead of the now-redundant XV-15 subsystem performance.

Phase I Design: Constrained Hybridisation of the XV-15

In Phase I, the XV-15 airframe is kept as close as possible to the historical configuration, except where the hybrid-electric propulsion system directly changes the aircraft. The purpose is not to produce the final Kestrel configuration, but to quantify what happens when hybrid-electric propulsion is introduced before any aircraft-level optimisation is allowed.

Within that constrained design space, a large amount of propulsive design options were developed in the form of a Design Option Tree (DOT). Seven of these architectures were retained as viable design candidates, a deliberately small amount: only architectures that could plausibly support a near-term, certifiable aircraft were deemed relevant, as the technology readiness objective in the RFP explicitly disfavours low maturity propulsion concepts. This led to a set of battery-based series and series-parallel architectures as the viable design space for Phase I, with the remaining variation concentrated on propulsion architecture, motor placement, turbine placement, and retention of the cross-shaft. Each architecture was evaluated at the minimum energy DoH of 10% (requirement SYS-1002), so that the ranking reflects the architecture choice rather than a different level of electrification.

The architecture options and the resulting weighted MCDA are shown in Table 4. The trade-off retains the criteria of Table 1 that meaningfully separate the candidate architectures at this level of fidelity: mission range, operating empty mass, and safety. Mission range receives the highest weighting as mission closure is the limiting Phase I problem, while empty mass and safety capture the principal penalties of the different component layouts and redundancy philosophies.

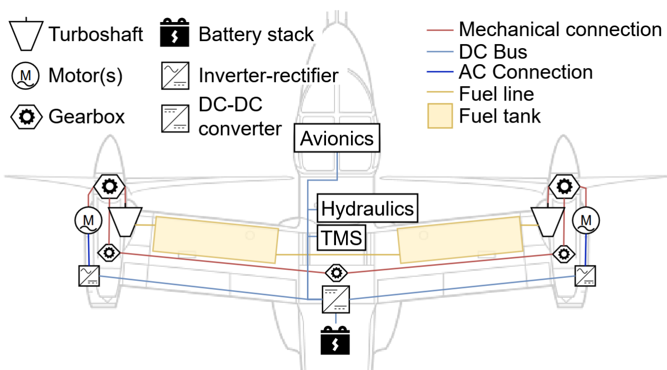

Figure 3: Selected Phase I PSC-7 series-parallel architecture. Turbines and electric motors are nacelle-mounted, while the cross-shaft is retained to preserve the XV-15 safety philosophy by providing mechanical redundancy, now alongside an electrical torque assist.

Table 4: Phase I architecture trade-off at 10% energy-based DoH. Each scored entry gives the raw value and the normalised value used in the weighted MCDA.

Arch.	OEM [kg]	Range [km]	Safety [-]	Final score
Weight [%]	25	50	25	**100**
PSC-1	5956.4 0.01	0 0.00	1.0 0.50	**13**
PSC-2	5877.8 0.05	0 0.00	1.0 0.50	**14**
PSC-3	4739.5 0.71	316 0.53	1.5 1.00	**70**
PSC-4	4744.6 0.71	319 0.53	0.5 0.00	**45**
PSC-5	5969.4 0.00	0 0.00	1.5 1.00	**25**
PSC-6	4233.3 1.00	597 1.00	0.5 0.00	**75**
PSC-7	4521.2 0.83	473 0.79	1.5 1.00	**85**

The Hybrid Energy Mass & Range Solver was used to evaluate each architecture under common DoH and fuel and battery sizing assumptions, with zero payload on-board. In this constrained Phase I setting, the solver then provides the achievable length of the cruise segment of the RMP for each candidate. The combination with the mass penalty of each architecture and qualitative redundancy assessments then allowed for all architectural design options to be compared on a consistent, integrated aircraft level. The MCDA trade-off resulted in the selection of the PSC-7 architecture, shown in Figure 3. Although PSC-6 gives a lower OEM and the longest computed range, it loses the safety benefit associated with the selected cross-shaft design, thereby making PSC-7 the favourable candidate. The Phase I aircraft-level specifications are reported in Table 11, which includes a 10% downsizing of the thermal engines paired with a 10% power DoH.

The Phase I result is limited: it identifies the most suitable constrained architecture, but shows that direct hybridisation of the XV-15 does not by itself recover useful payload-range capability. With the original VTOL mass constraint retained, batteries, motors, inverters, cabling, and thermal-management equipment consume the mass margin otherwise available for payload. Phase I therefore becomes the reference failure mode for Phase II: the PSC-7 architecture is retained as the conceptual propulsion basis, while aircraft-level sizing is reopened to optimise wing efficiency, proprotor efficiency, structural mass recovery, and energy-storage loading together.

Phase I to Phase II Design Strategy

The central failure mode of direct hybridisation, highlighted by the Phase I performance, warrants the design to be reviewed before the Phase II development commences. In particular, changes should be made where the Phase I limitation is most direct: mass and power.

The XV-15 Short Take-Off (STO) MTOM of 6804 kg (15,000 lb) is adopted as the Phase II VTOL design mass without increasing its STO mass limit, since the legacy aircraft is already structurally rated for that mass level. This increase therefore does not require a structural overhaul. The thermal engines are additionally no longer downscaled; instead, the original T53-class turboshafts are retained and the supplementing electrical assist is resized for a 15% *power* DoH. This provides the necessary power for vertical take-off at the new VTOL MTOM. Together, these three design choices lead to the restoration of the required 726 kg (1600 lb) payload mass, such that the remaining mass margin can be allocated to fuel and modular battery energy storage.

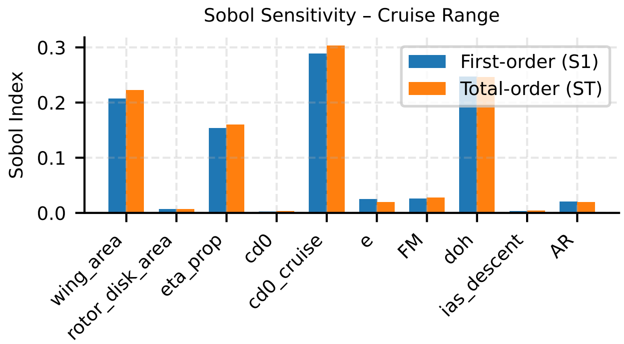

(a) Cruise-range sensitivity.

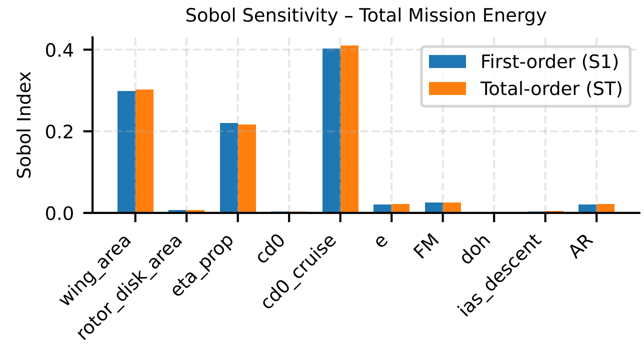

(b) Total mission energy sensitivity.

Figure 4: Sobol sensitivity results for the updated Phase I mass-and-range model. First-order and total-order indices identify cruise drag, wing reference area, and propulsive efficiency as the highest-leverage optimisation parameters.

The updated baseline restores payload carrying capabilities, but still has room for improvement in the dated, legacy subsystems. The remaining question is thus where optimisation efforts should be spent to increase payload-range capabilities most efficiently whilst limiting the resulting development budget. A broad redesign of every subsystem would be inconsistent with the cost and certification logic of the Kestrel. The Phase II optimisation process is therefore guided by a Sobol sensitivity analysis of the Hybrid Energy Mass & Range Solver, performed before subsystem optimisation. This allowed for the identification of the design variables with the strongest influence on cruise range and required mission energy.

The Sobol analysis varies each design parameter $\pm$100% around its nominal value, whilst simultaneously sampling the others using Saltelli sampling. This allows for the output variance to be decomposed into first-order effects and total-order effects, retaining both direct sensitivities and interactional ones . The result is shown in Figure 4. Cruise zero-lift drag c_{d_0} is the dominant driver, whilst wing reference area A and propulsive efficiency η_{prop} are the next most relevant contributors. Hover Figure of Merit FM has a smaller but still relevant influence once the length of the vertical segments are increased, whereas DoH mainly presses payload-range performance due to the unfavourable energy density of the batteries. The remaining parameters have comparatively low influence on the performance. The Phase II strategy therefore concentrates the redesign on cruise aerodynamic efficiency, proprotor efficiency, and structural mass reduction, whilst treating battery mass as an optimisation lever to maximize the the energy DoH for the RMP.

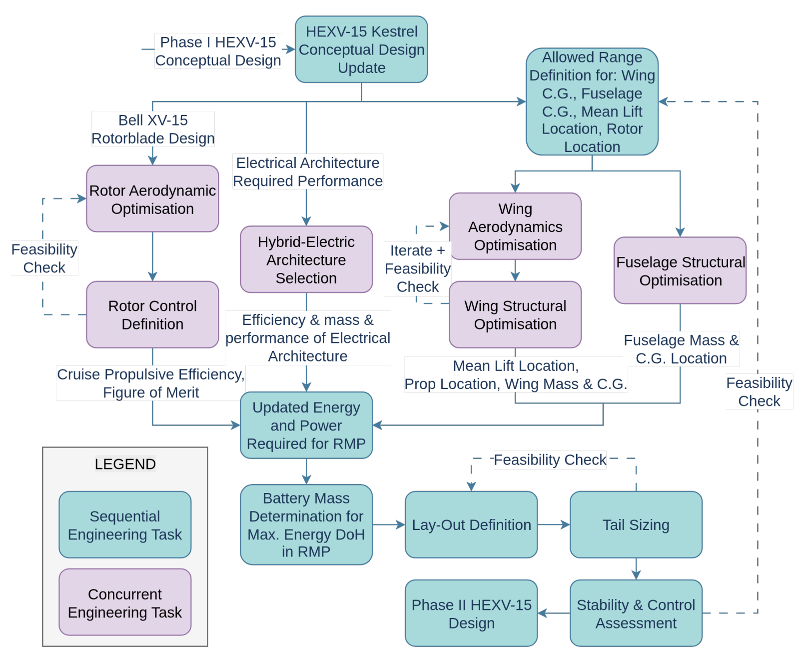

Figure 5: Phase II preliminary design strategy. Hybridisation is treated as a coupled aircraft-level optimisation problem, with proprotor, wing, structures, electrical architecture, control and integration feeding back into the final configuration.

The resulting design strategy, featuring concurrent engineering principles, is shown in Figure 5. Wing optimisation is used to reduce the dominant cruise energy term, whereas the fuselage outer mold is retained to maximise the design heritage. Proprotor optimisation reduces shaft-power demand in hover and cruise, and structural mass recovery offsets the hybrid-electric installation mass penalty. The hybrid-electric architecture is then re-sized from the baseline to match the (lowered) demands of the optimised aircraft, rather than being imposed from the original constrained Phase I case. This allows for modular battery loading, final energy-storage sizing, control integration, performance assessment, sustainability analysis, and cost evaluation to converge on a single Phase II configuration.

Aerodynamic Optimisation: Wing Extensions for Performance Recovery

Cruise is the range-driving segment of the RMP, so wing aerodynamic efficiency is a first-order payload enabler. To support this design step, a dedicated aerodynamic optimisation tool was developed for both the wing and proprotor optimisation. The tool couples DUST , used as the mid-fidelity aerodynamic solver, with NSGA-II for multi-objective black-box optimisation , implemented through Optuna . DUST is appropriate at this design stage as it captures lifting-surface and wake effects at a computational cost suitable for repeated candidate evaluations, whereas full RANS/URANS optimisation would computationally be too expensive for the desired design space exploration. NSGA-II is employed as the problem is bounded, non-linear, multi-objective, and not available in closed analytical form. The integrated tool can therefore provide a Pareto front of optimised aerodynamic designs within prescribed geometric and operational bounds, whilst retaining design diversity across the competing objectives; all without requiring gradient information.

Two wing geometry routes were considered. First, the main wing was optimised within bounded geometric limits to retain XV-15 design heritage and avoid excessive changes to the fuselage, nacelle interface, and stability characteristics. Second, a novel nacelle-mounted wing extension was introduced to recover cruise efficiency without increasing the total rotor tip-to-tip span, thereby remaining compatible with SYS-1201. The extension rotates with the nacelle, reduces the need for large inboard-wing changes, and increases effective aspect ratio in wing-borne flight. The optimisation was performed for both the bounded basic-wing configuration and the combined extended-wing configuration, employing similar design bounds.

Table 5: Wing trade-off matrix for the Pareto-front candidates. The selected E17 wing scores highest because the cruise-efficiency gain outweighs its mass and bending-moment penalties while retaining a derivative inboard-wing geometry.

	ID →	W-001	W-002	W-003	W-004	
	Criterion	L/D [-]	Legacy Score [-]	Mass [kg]	Bending Moment [kNm]	
	Weight % →	50	12.5	25	12.5	Score ↓
Basic Wing	B25	0.74 25.92	0.92 3.29	1.00 250.24	1.00 137.50	**86**
	B26	0.75 26.21	0.67 2.40	0.93 270.03	0.98 140.03	**81**
	B9	0.77 26.88	0.80 2.85	0.99 253.80	0.96 142.82	**85**
	B11	0.81 28.32	0.60 2.13	0.94 265.60	0.93 147.28	**83**
Extended Wing	E45	0.83 29.06	0.60 2.12	0.85 297.65	0.79 173.45	**80**
	E46	0.88 31.07	0.83 2.96	0.84 297.65	0.75 182.31	**85**
	E26	0.93 32.72	0.57 2.02	0.85 295.49	0.73 189.43	**84**
	E13	0.98 34.34	0.66 2.34	0.85 295.85	0.70 195.18	**87**
	E17	1.00 35.11	1.00 3.57	0.84 298.29	0.70 196.94	**92**

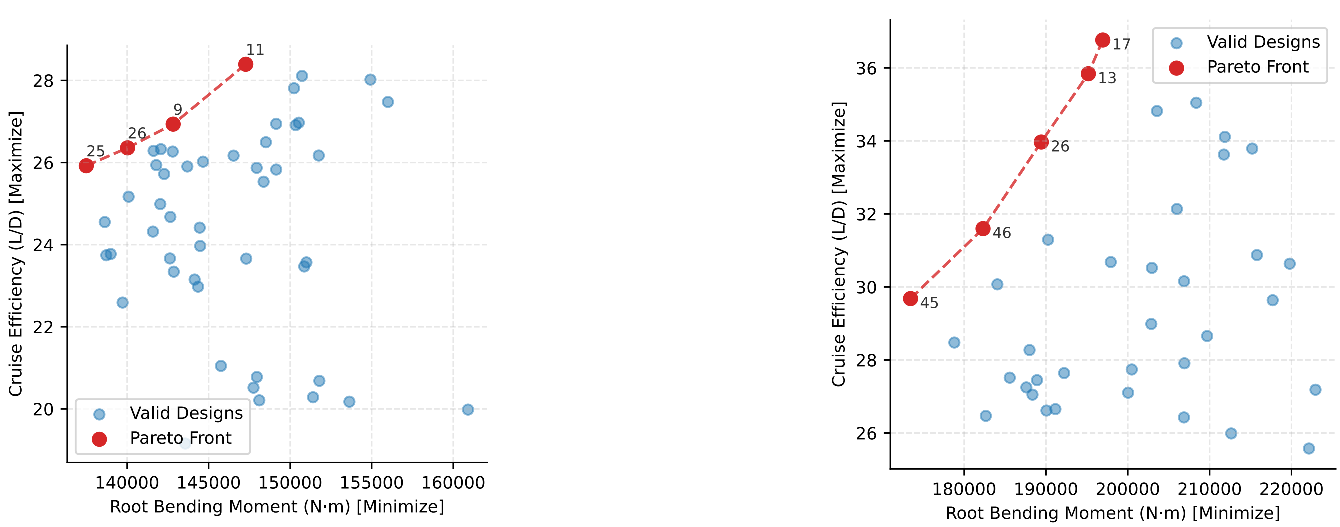

(a) Basic-wing (BW) Pareto front.

(b) Extended-wing (EW) Pareto front.

Figure 6: Wing optimisation Pareto fronts showing the basic-wing and extended-wing candidates for the final MCDA.

The optimisation resulted in separate Pareto fronts for the basic-
wing and extended-wing design spaces, shown in Figure 6. Candidate wings were trimmed to the cruise lift requirement before final performance evaluation, ensuring that the reported lift-over-drag L/D corresponds to the actual RMP cruise operating point rather than an arbitrary angle of attack. Pareto-front candidates were then passed into the weighted trade-off in Table 5. Performance was quantified by clean-wing L/D at the trimmed cruise condition, mass by the structural mass method used in the structural optimisation branch, cost by the root bending moment as a first-order structural-cost driver, and legacy retention by the normalised geometric deviation from the XV-15 inboard wing, including a penalty for the outboard extension.

This resulted in the selection of the E17 extended wing design candidate, as it presents the best weighted balance between range recovery and development risk. Its clean-wing performance is shown in Figure 7, where the lift curve, drag polar, and efficiency curve demonstrate the improved cruise operating point relative to the baseline XV-15, evaluated in DUST. The corresponding geometric and aerodynamic quantities are summarised in Table 6.

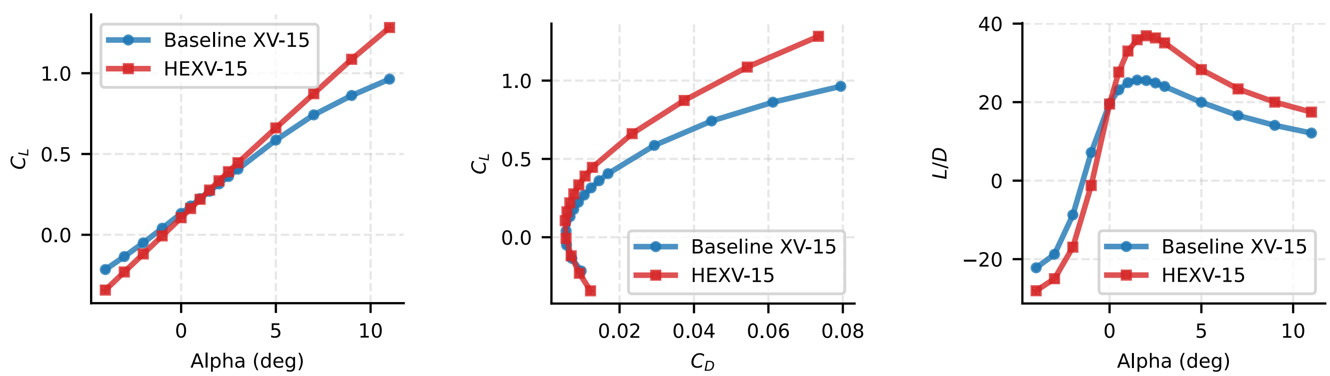

(a) Lift curve. **(b)** Drag polar. **(c)** L/D curve.

Figure 7: Clean-wing aerodynamic comparison between the baseline XV-15 and the HEXV-15 wing. Inclusion of the wing extension is a key design decision for the cruise energy reduction of the Phase II aircraft.

Table 6: Final clean-wing aerodynamic and geometric characteristics.

Parameter	**XV-15**	**HEXV-15**	**Change**	**Relevance**
Main wingspan, m (ft)	9.80 (32.2)	9.84 (32.3)	+0.3%	XV-15 inboard wing span is negligibly increased.
Nacelle extension span, m (ft)	–	2.31 (7.6)	–	Additional lifting surface is added outboard of each nacelle without exceeding the rotor tip-to-tip span constraint.
Wing area, m^2 (ft^2)	15.68 (169)	19.98 (215)	+27.4%	Lower lift coefficient at the design condition.
Aspect ratio, –	6.12	10.40	+70.0%	Lower induced drag in wing-borne cruise.
Oswald efficiency, –	0.703	0.712	+1.3%	Wing lift distribution benefits are retained.
Wing incidence, deg	3.00	1.80	-40.0%	Lower trim incidence at cruise.
Clean-wing L/D, –	23.40	35.10	+50.0%	Primary cruise energy reduction result.
Cruise C_L, –	0.3929	0.3083	-21.5%	Lower lift coefficient for the same mission condition.
Cruise C_D, –	0.0167	0.0088	-47.0%	Direct drag reduction at the cruise design point.
Aircraft-level C_{D0}, –	0.033	0.027	-18.2%	Lower drag input for payload-range modelling.

Proprotor optimisation: Efficiency Recovery

The proprotor redesign uses the same aerodynamic optimisation tool as the wing optimisation, now applied to the isolated rotor blade geometry at the hover and cruise operating points. The optimisation scope is deliberately focused on the blade geometry only: the three-bladed XV-15 architecture, hub, shaft, gearbox interface, control mechanisms, and nacelle installation are retained. This preserves the derivative-aircraft logic of the Kestrel whilst still targeting the rotor variables that most directly affect the hover Figure of Merit (FM), cruise propulsive efficiency η_{prop}, and consequently the hybrid-electric architecture sizing. An improved design results, with space left for optimisation of its surrounding architecture in further development efforts.

The focus thus lies on the blade radius, chord distribution, twist distribution, sweep, collective pitch and rotational speed, which are allowed to vary within bounded limits. The optimisation considered 394 acceptable proprotor candidates, generated through NSGA-II and trimmed for both cruise and hover operation through an estimator. Simulations of these candidates in DUST showed 53 designs to pass the stringent thrust and required shaft power constraints. The accepted candidates produced a Pareto front of four designs in the hover and cruise efficiency space, as shown in Figure 8. To include a larger set in the trade-off, three additional high performing candidates were retained based on their weighted combined hover and cruise performance, giving seven unique candidates for the final rotor trade-off.

The trade-off, shown in Table 7, applies the programme objectives at rotor level. Performance is quantified through a normalised and weighted combined efficiency using hover Figure of Merit and cruise propulsive efficiency, with the weighting reflecting the RMP energy distribution between vertical and wing-borne flight. Complexity is estimated from the normalised deviations in twist, sweep, and chord taper relative to the baseline XV-15 proprotor, thereby penalising geometries that move further away from the base design. Mass is estimated from blade volume, as a detailed structural design is outside the scope of this design. Hover noise is estimated with a tip-Mach scaling law, providing a consistent relative comparison without requiring a full acoustic footprint for every candidate .

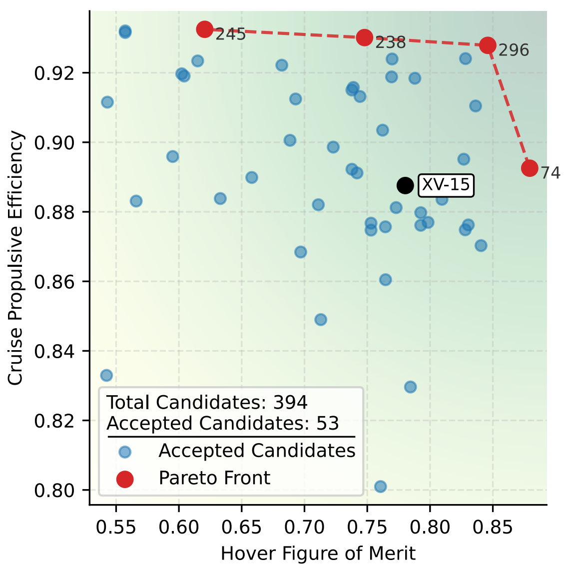

Figure 8: Proprotor optimisation Pareto front. Candidates are screened against thrust, power, geometry, and operating constraints. The Pareto-front candidates expose the hover and cruise efficiency trade-off before final selection.

Table 7: Proprotor trade-off matrix for the selected blade candidates. Blade 296 is selected because it provides the best weighted compromise between cruise efficiency, hover figure of merit, mass, complexity, and relative hover noise score.

	ID →	R-001	R-002	R-003	R-004	
	Criterion →	Performance	Complexity	Mass	Noise	
	Weight % →	55	25	10	10	Score ↓
Rotor Blades	XV-15	0.00	1.00	0.70	0.60	**38**
	74	0.86	0.25	0.00	1.00	**63**
	236	0.91	0.11	0.21	0.52	**60**
	238	0.89	0.04	0.69	0.20	**59**
	245	0.83	0.05	1.00	0.00	**57**
	261	0.91	0.00	0.37	0.00	**54**
	296	1.00	0.20	0.32	0.14	**64**
	395	0.94	0.20	0.17	0.39	**62**

Blade 296 obtains the highest combined score and is therefore selected for the Phase II HEXV-15 design. Its performance is driven by a favourable redistribution of chord and twist: its reduced tip chord limits loading and flow acceleration in the generally high-velocity outer blade region, whilst the increased mid-span chord moves the main thrust generation towards a more efficient portion of the blade. Its milder twist distribution reduces inefficient inboard loading in hover. The selected operating schedule also separates hover and cruise rotational speeds more strongly than the XV-15 baseline. Although this improves the design-point efficiencies, it also introduces aeroelastic considerations that need further investigation.

Table 8: Phase II HEXV-15 proprotor design specifications, compared to the legacy XV-15 design.

Metric	**XV-15**	**HEXV-15**	**Design consequence**
Radius, m (ft)	3.81 (12.5)	3.74 (12.3)	Remains within the 25 ft diameter constraint.
Number of blades	3	3	Retains RFP blade-number constraint and XV-15 architecture.
Isolated cruise η_{prop}	0.888	0.928	Higher useful cruise thrust per shaft power.
Isolated hover FM	0.780	0.850	Lower hover shaft power for the same thrust.
Installed cruise η_{prop}	0.858	0.919	6.7% installed cruise efficiency increase.
Installed hover FM	0.603	0.718	16.0% installed hover efficiency increase.

Continued on next page

Metric	XV-15	HEXV-15	Relevance
Cruise / hover speed, rad/s	54.2 / 61.4	32.7 / 65.0	Efficient operating split; requires aeroelastic and drivetrain assessment.
Cruise / hover collective, deg	41.5 / 8.5	53.8 / 3.0	Operating point shift stemming from changes in twist distribution.

The isolated proprotor performance curves in Figure 9 show that the selected blade improves the relevant hover and cruise operating points while retaining trends consistent with XV-15 reference behaviour over various blade loading values. The main specifications of the optimised blade and a comparison with the legacy design are shown in Table 8, including simple estimations of the installed efficiencies. This links the isolated aerodynamic result to an aircraft-level energy recovery.

The result represents a strong preliminary design candidate, though not yet a final optimum: candidate generation neglects rotor-wing, rotor-nacelle, fuselage, and conversion interaction effects, which are only represented later through simple installation corrections. Higher-fidelity installed aerodynamics, aeroelasticity, whirl-flutter, vibration, drivetrain dynamics, and control coupling are next-stage validation items, and the wing extension may shift the favoured proprotor design. At preliminary level the result is nevertheless directly useful: the improved hover FM and cruise η_{prop} reduce shaft-power demands throughout the RMP, making the proprotor redesign a payload enabler that offsets the hybrid-electric mass penalty.

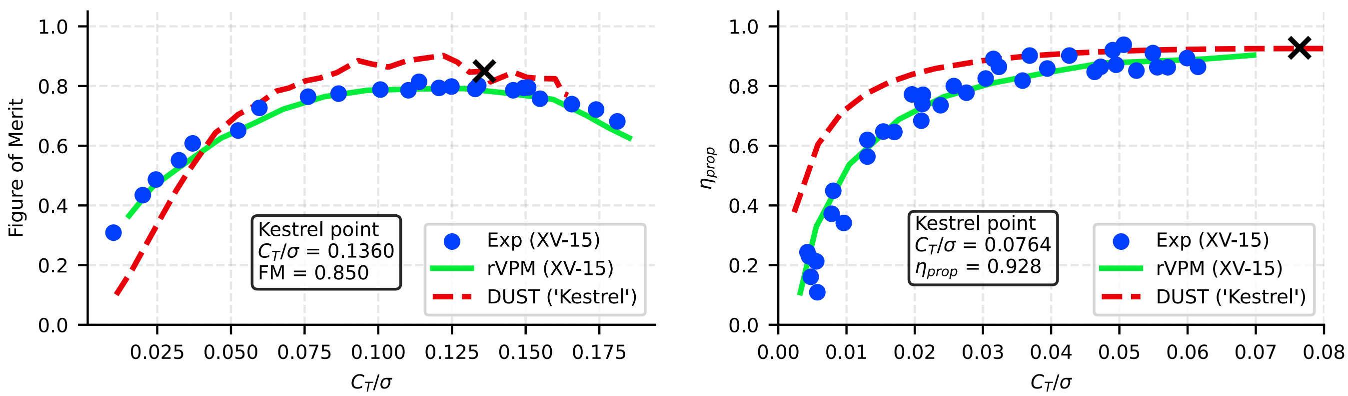

(a) Hover Figure of Merit.

(b) Cruise propulsive efficiency.

Figure 9: Isolated proprotor performance compared with XV-15 reference data . The selected design improves the mission operating points while remaining within the inherited geometric constraints.

Structural Optimisation and Mass Overview

Structural optimisation is the final aircraft-level task used to recover payload-range capability lost during hybridisation. After the wing and proprotor redesigns reduce mission energy demand, the structural task attacks the remaining problem directly: empty mass. Completed mass properties are then passed to the system-integration loop for control and stability margins, hybrid-electric architecture definition, and final battery sizing closure.

The wing is re-sized from the loads to provide a justified mass estimation, needed to supplement the optimised wing outer mould design. Manoeuvre, gust, and jump take-off cases, stemming directly from EASA certification and the concept of operations , are evaluated across the relevant aircraft mass states. The critical spanwise shear, bending, and torsional loads are then used to size a closed, two-spar composite wingbox with stiffened skins. A carbon/epoxy construction with Omega stringers is selected for mass efficiency, stiffness, buckling resistance, and manufacturability. The wingbox is then optimised bay-by-bay: skin thickness, cap area, web thickness, and stringer count are varied to minimise mass while satisfying stress, shear, buckling, nacelle-deflection, and twist limits. This reduces the structural wing mass from 396 kg (873 lb) to approximately 275 kg (606 lb), a 121 kg (267 lb) saving, as seen in **??**.

The fuselage and empennage are treated more conservatively. Because a full, detailed fuselage redesign is outside the current scope of the Phase II design, the savings are estimated from composite aircraft structure literature . This step remains credible as the fuselage outer mould is unchanged compared to the XV-15 baseline, and because the Phase II VTOL MTOM is capped at the original XV-15 STO mass level. As resizing the tail also doesn't impose significant changes in geometry and loads, the statistical weight estimation by imposing composite materials remains credible as well.

fundamentally higher than the legacy case. This gives a 26% reduction for both fuselage and empennage, reducing them from approximately 654 kg (1442 lb) to 484 kg (1067 lb), and from approximately 95 kg (209 lb) to 70 kg (155 lb), respectively. A smaller contribution is obtained from the rotor and driveline: composite blade assumptions and cross-shaft resizing provides only a marginal saving of 17 kg (37 lb), whilst still retaining the cross-shafted safety philosophy.

The primary structural savings relative to the XV-15 baseline therefore amount to approximately 318 kg (701 lb), or 27.2%. The savings are summarised in Figure 10. This mass recovery is a direct part of the mechanism that makes the final hybrid-electric sizing viable: the aircraft can accept a 1303 kg (2873 lb) design-point battery mass because the structural recovery, rotor efficiency, wing efficiency, and MTOM update together create payload closure.

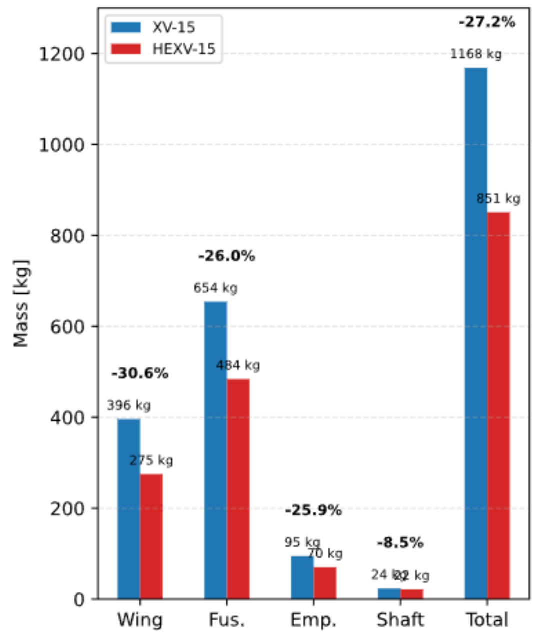

Figure 10: Primary structural mass recovery relative to the XV-15 baseline.

Hybrid-electric Architecture and Battery Performance

With subsystem-level mass recovery and efficiency improvement established, the hybrid-electric system is sized as an integrated part of the Phase II aircraft rather than an isolated retrofit. The architecture retains the Phase I series-parallel logic: nacelle-mounted turboshafts and electric engines, a retained cross-shaft for mechanical redundancy, and electrical torque assist scheduled across mission segments with emphasis on high-power-demand phases. The difference is that the battery system and electrical architecture are now sized around the optimised Phase II aircraft, whose wing and proprotor improvements lower power demands and thus electric componentry mass.

This sizing is based on real component selection through trade-offs of Commercial Off-The-Shelf (COTS) components. Candidate motors, inverters, high-voltage cabling, and cells were screened through component-level performance, resulting in the Helix SPC242-110 motor, Helix MCU1200-1050 inverter, Huber+Suhner RADOX 155 HVDC cable, and Molicel INR-21700-P45B cell as the preliminary electrical chain. These selections provide the mass, volume, voltage, resistance, and power limits used in battery sizing and loss calculations .

The Hybrid-Electric Mass and Range Solver is used to determine the feasible DoH–range design space and identify the design-point satisfying the 500 km (311 mi) RMP requirement within MTOW constraints. This sizing is, however, not only driven by the required mission energy: battery internal losses, distribution losses, thermal limits, ageing, Depth of Discharge (DoD) and the related degradation all affect the usable energy available over the required service life. The sizing problem is therefore a balance: a larger battery reduces DoD and cell stress but increases aircraft mass, whereas a smaller battery improves payload-range performance but accelerates ageing, thereby increasing acquisition costs related with pack replacement. Estimation of these losses are thus pertinent before the final battery mass can be calculated.

For the final design-point, two Helix SPC242-110 motors provide up to 684 kW (917 hp) of electrical assist. Relative to the peak propulsion power requirement of approximately 2430 kW (3259 hp) , this corresponds to a maximum power hybridisation of 28.1%. The design-point selected by the Hybrid-Electric Mass and Range Solver achieves an energy hybridisation (DoH) of 18% while satisfying the 500 km (311 mi) RMP requirement within MTOW constraints. The electrical system remains distributed over two nacelle branches connected through a 950 VDC high-voltage architecture. Using the selected RADOX 155 cable properties, the peak HVDC cable loss is only 0.177 kW (0.24 hp), or 0.051% of transmitted electrical power. Integrated over the full RMP, cable losses remain below 0.27 MJ (0.10 hp h) and are therefore negligible compared with propulsion energy. The limiting electrical design constraints are consequently battery internal loss, pack temperature, ageing, and allowable DoD, as summarised in Table 9.

Three representative electrical operating envelopes were evaluated to quantify the effect of electrical scheduling on loss and ageing during the battery sizing process, as shown in Figure 11b. Envelope A uses electrical assist in VTOL, hover, climb, and landing, delivering 196.6 MJ (73.2 hp h) with 15.86 MJ (5.91 hp h) of battery loss and an integrated electrical efficiency of 0.870. Envelope B adds limited cruise assist, delivering 437.9 MJ (163.1 hp h) with 8.54 MJ (3.18 hp h) of battery loss and 0.923 efficiency. Envelope C assumes full-phase electrical availability, delivering 890.7 MJ (331.8 hp h) with 9.19 MJ (3.42 hp h) of battery loss and 0.931 efficiency. The result is that broader, lower-stress electrical use can be more efficient than short, high-intensity extraction, provided that pack temperature is controlled.

Table 9: Electrical and battery design quantities relevant to the Phase II design point.

Quantity	**Value**	**Design relevance**
Architecture basis	PSC-7	Series-parallel nacelle-mounted torque assist with retained cross-shaft.
Motor / inverter	Helix SPC242-110 / MCU1200-1050	Off-the-shelf basis for power, mass, and volume sizing.
HVDC cable / cell	RADOX 155 / Molicel P45B	Basis for cable-loss and battery-loss estimation.
HVDC bus voltage	950 V	Limits current and resistive losses at the required assist power.
Peak electrical assist power	684 kW (917 hp)	Provides 28.1% power DoH at RMP take-off.
Peak HVDC branch current	182.5 A	Drives cable and protection sizing.
Peak cable loss	0.177 kW (0.24 hp)	Only 0.051% of transmitted electrical power.
Design battery mass	1303 kg (2873 lb)	Main energy-storage mass for the 18% DoH RMP design point.
Design DoD / temperature	71% / 20 °C (68 °F)	Balances mission energy extraction against ageing and thermal limits.
Predicted battery lifetime	4.08 years	Meets the four-year target at two missions per day.
Thermal approach	Liquid cooling loop	Enables repeatable operation and pack-temperature control.

The DoD and operating temperature ageing relation is the last, but very relevant, part of the sizing logic, and is shown in Figure 11a. Higher DoD reduces the installed battery mass required for the RMP, improving payload-range performance, but it increases cyclic degradation and reduces replacement interval. Lower DoD has the opposite effect: it improves lifetime margin but adds battery mass that must be carried through every mission. The selected 71% DoD at a 20 °C (68 °F) operating temperature presents a compromise between RMP closure, four-year battery lifetime for two missions per day, and an acceptable installed mass. The Kestrel is therefore not sized around maximum single-mission battery extraction, but around repeated commercial operation: stable pack temperature, predictable ageing, and a maintenance cycle compatible with AAM service .

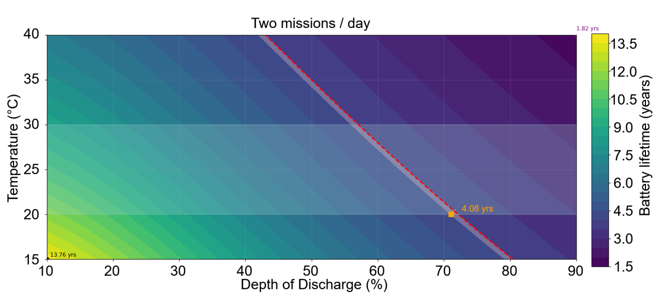

(a) Battery lifetime as a function of DoD, operating temperature for two missions per day.

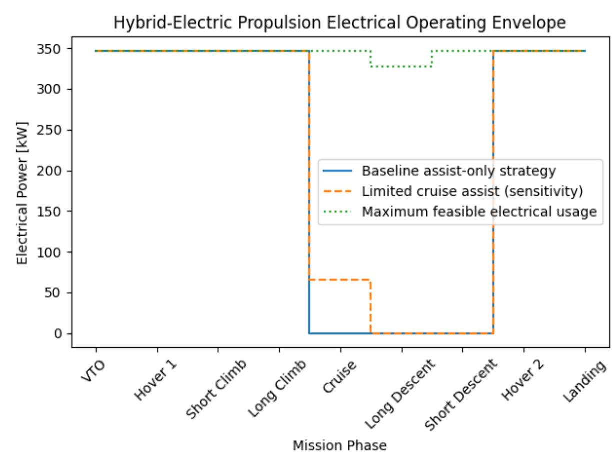

(b) Electrical operating envelopes.

Figure 11: Battery ageing and electrical scheduling considerations. The selected design point uses approximately 71% DoD at 20 °C (68 °F), giving a predicted lifetime of 4.08 years at two missions per day.

Lastly, a key design aspect of the HEXV-15 Kestrel is the modular battery design, which is treated as a mission-flexible energy system. The final design-point employs twenty identical removable battery packs (226s4p), allowing the operator to adjust installed battery capacity and Degree of Hybridisation according to mission demands while maintaining a fixed electrical architecture. This modularity is important operationally: the aircraft is not forced to carry one fixed battery mass for every mission, and turnaround can be based on pack replacement rather than slow full-aircraft charging. The architecture therefore provides flexibility in balancing payload, range, and hybridisation level without requiring propulsion-system modification.

Phase II Design Integration and Payload-Range Analysis

The wing, proprotor, and structural optimisations are paired with the selected hybrid-electric architecture to close the aircraft as one integrated system. The Hybrid-Electric Mass and Range Solver combines these elements and finds the total battery mass required for maximisation of the energy-based DoH at the RMP design point, including compliance with payload, crew and fuel requirements. The result is the finalised Phase II HEXV-15 Kestrel configuration: 726 kg (1600 lb) payload, 18% DoH, approximately 1303 kg (2873 lb) of battery mass, and 415 kg (915 lb) of fuel.

The subsystem-level efforts have thus resulted in a feasible full aircraft definition of the HEXV-15 Kestrel. The integrated vehicle is shown in a three-view drawing at the end of this document, including the optimised wing with nacelle-mounted extensions, redesigned proprotors, updated structural layout (not visible), and hybrid-electric installation. The passenger seating and battery pack arrangement are additionally visible. The battery packs are positioned as close as practical to the aircraft centre of gravity to minimise their impact on stability and control. Note that the horizontal tail sizing was performed with the battery-driven centre-of-gravity envelope included in the design space.

The payload-range diagrams in Figure 12, Figure 13, and Figure 14 provide an aircraft-level performance assessment of the integrated Phase II design. Under the same RMP modelling assumptions, the XV-15 baseline carries approximately 755 kg (1665 lb) of payload, but does so without hybrid-electric energy storage and thus has space left in its fuel tank. The updated Phase I pre-optimisation aircraft is a more relevant intermediate reference than the initial version: it allows for direct quantification of the effects of subsystem-level optimisation on the integrated vehicle, whilst still showing that hybridisation alone cannot provide the required payload-range performance without the subsequent optimisation phases. At the design point of 18% hybridisation, it can close the RMP only with a shortened range of 337 km (209 mi). The final Phase II HEXV-15 closes the RMP at the required 726 kg (1600 lb) payload and selected 18% DoH, while retaining range flexibility; when payload is no longer the sizing condition, the zero-payload ferry capability reaches approximately 916 km (569 mi). The original constrained Phase I aircraft is deliberately not repeated in the payload-range comparison because it cannot execute the RMP with the required payload on board.

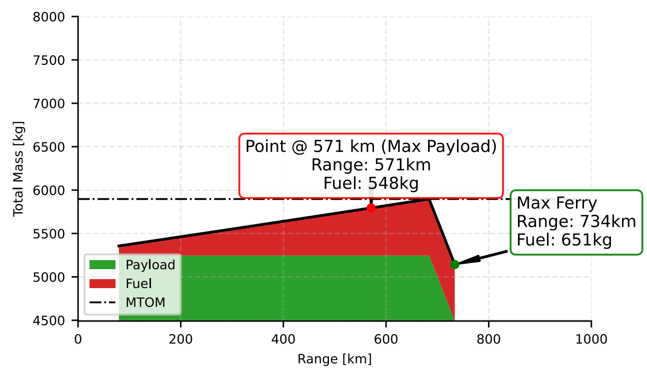

Figure 12: Payload-range comparison under RMP assumptions for the baseline XV-15.

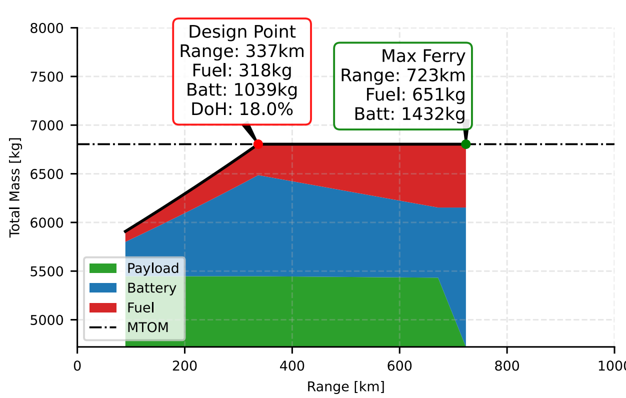

Figure 13: Payload-range comparison under RMP assumptions for the updated Phase I, pre-optimisation aircraft. The original constrained Phase I aircraft cannot carry the RFP payload on the RMP, so it is not included in this assessment.

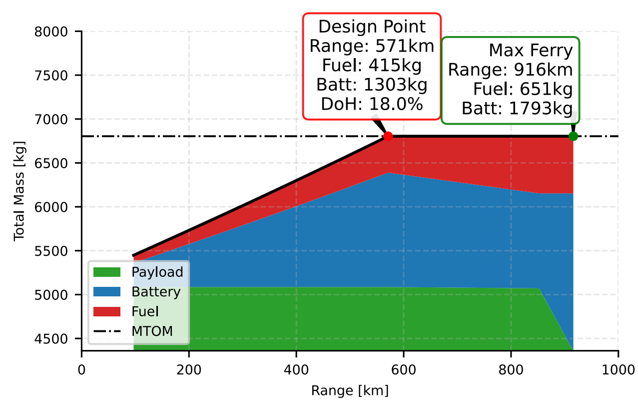

Figure 14: Payload-range diagram under RMP assumptions of the Phase II HEXV-15 Kestrel. The design builds on the recovered 726 kg payload stemming from the Phase I update, and extends the design-point range to RMP value.

The modular battery design can then be leveraged to show the true operational range of the aircraft and the true flexibility of its hybridisation capability; providing relevant operational benefits compared to the legacy XV-15. Two complementary analyses are used. First, Figure 15a shows the maximum ferry range obtained for selected battery loadings in an adjusted RMP comparison case, where the hover phases are now removed. This demonstrates the absolute range capability of the system, with the 17% energy DoH configuration providing a maximum of approximately 1016 km (631 mi). Second, Figure 15b shows the dispatch-planning trend for the complete RMP definition, where only the cruise segment length is varied and the maximum feasible DoH is solved for each total mission length. This gives a maximum extended RMP cruise segment of approximately 785 km (488 mi) near 10% DoH. Higher battery loading increases the electrical fraction, but progressively displaces fuel and therefore reduces range. The selected 18% design point is consequently the maximum feasible DoH for the required 500 km (311 mi) *cruise* segment of the *nominal* RMP with payload, hover segments, battery-life considerations, and fuel requirements simultaneously satisfied.

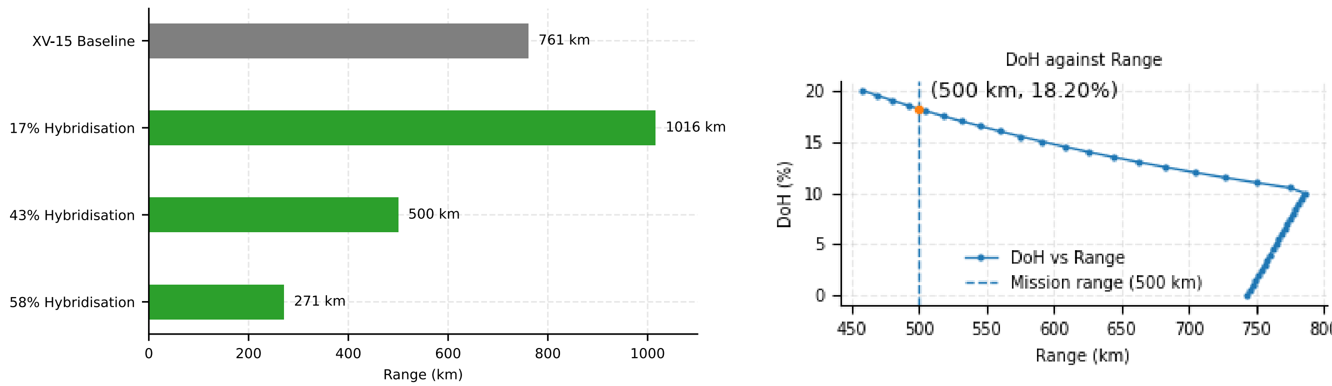

(a) Maximum ferry range at selected DoH configurations.

(b) RMP *cruise segment* length versus maximum feasible DoH for modular dispatch planning.

Figure 15: Modular battery loading turns DoH into an operational variable. The no-hover ferry comparison gives approximately 1016 km (631 mi) at 17% DoH, 500 km (311 mi) at 43% DoH, and 271 km (168 mi) at 58% DoH, while the full-RMP dispatch trend reaches its maximum cruise segment length of approximately 785 km (488 mi) near 10% DoH. The selected design point remains 18% DoH for the complete dispatch-to-dispatch RMP with the required payload.

Flight Envelope, Power Curve, and Conversion Corridor

The payload-range analysis has proven the energy balance of the Phase II aircraft, but the integrated Kestrel must also retain the rotor-borne, conversion, and wing-borne margins that make the XV-15 architecture operationally valuable. This is assessed with a coupled low-order performance model, as the intent is to prove retention of tiltrotor qualities rather than a detailed analysis. Rotor-borne power required is estimated with blade-element momentum theory combined with actuator-disk relations, while aeroplane-mode power required is obtained from the fixed-wing drag polar. Available turboshaft power is scaled with altitude, while the electrical torque-assist contribution is retained as part of the hybrid-electric power margin. Sweeping velocity, altitude, and nacelle angle with this model gives the envelope and power-curve results in Figure 16. The Phase II HOGE ceiling is found where out-of-ground-effect hover power required at VTOL MTOM equals available power, giving 3014 m (9888 ft). Applying the ground-effect correction gives a HIGE ceiling of 3568 m (11,706 ft). The Phase II aeroplane-mode service ceiling is obtained from the altitude at which the wing-borne power margin closes, resulting 9799 m (32,149 ft). The corresponding XV-15 values are 2637 m (8652 ft), 3200 m (10,499 ft), and 8800 m (28,871 ft), respectively .

Flight dynamics models are also made to check the structural and conversion implications of the Phase II geometry, resulting in Figure 17. The V-n diagram is generated by trimming the three-degree-of-freedom longitudinal model and applying manoeuvre and gust perturbations: elevator step inputs provide the manoeuvre loads, while vertical-speed perturbations provide the gust loads. The conversion corridor is obtained by gridding nacelle angle and forward speed, imposing steady level conditions, and solving the trim problem for thrust, pitch attitude, and elevator deflection; points are retained only where a trimmable condition is found. This links the wing extension, rotor optimisation, and hybrid-electric power margin to the actual operating modes of the vehicle rather than treating them as isolated subsystem gains.

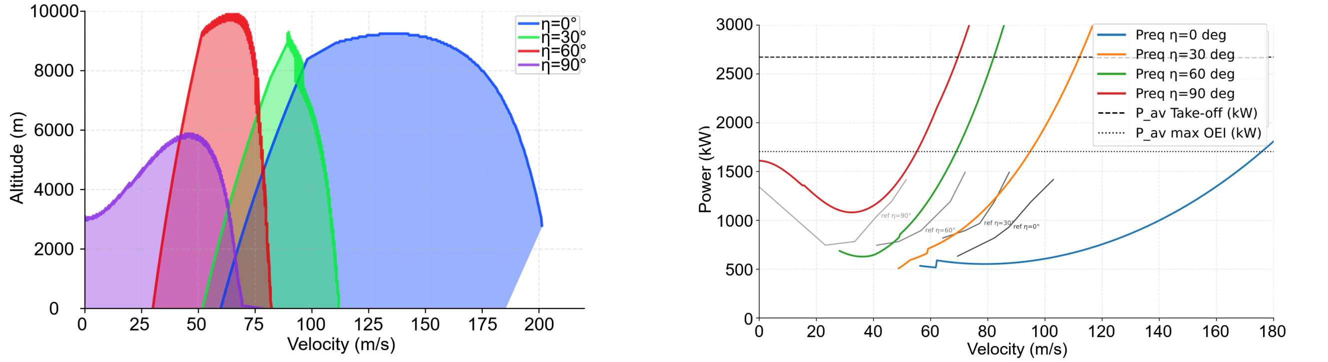

(a) Flight envelope by nacelle angle, giving maximum velocity as a function of altitude in ISA conditions.

(b) Power required and power available as a function of velocity. For sea level conditions.

Figure 16: Preliminary aircraft performance envelope. The power curve is generated from nacelle-angle-dependent rotor and wing-borne power estimates, while the envelope retains the velocity-altitude combinations for which available hybrid-electric power exceeds required power.

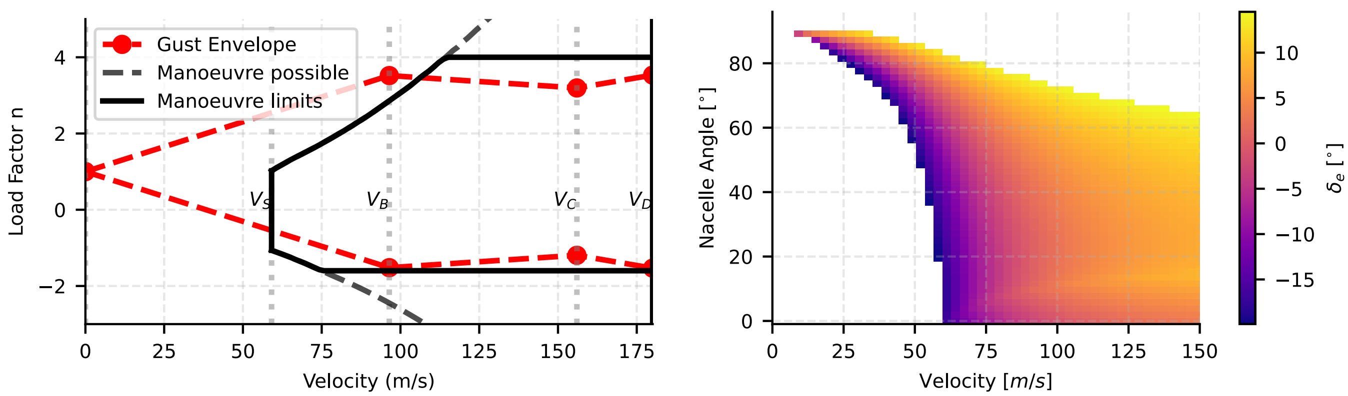

(a) Phase II V-n diagram.

(b) Phase II conversion corridor.

Figure 17: Structural and conversion behaviour. The V-n diagram is obtained from trimmed three-degree-of-freedom manoeuvre and gust simulations, while the conversion corridor maps the nacelle-angle and forward-speed combinations for which the Phase II aircraft remains trimmable and stable.

The results in Figure 16 and Figure 17 show that the Phase II redesign improves wing-borne performance and preserves vertical-flight capability, but also clarifies the remaining certification-relevant sensitivities. The larger wing area and span increase the relevance of gust loading, although manoeuvre loads change less strongly and remain compatible with the retained +4/-1.6 load-factor limits. The conversion corridor remains open, but narrows above approximately 60° nacelle angle, where off-nominal gusts, weight growth, or degraded electrical capacity could erode margin. The next validation step should therefore combine six-degree-of-freedom conversion dynamics, gust modelling, nacelle-angle scheduling, and electrical-assist scheduling to further investigate these effects.

Sustainability Analysis: Emissions, Noise, and RPM Scheduling

Hybridisation is pursued primarily to reduce the climate impact of the vehicle during operation, matching the general AAM trend of sustainable aviation. When combined with noise-aware rotor operation, it also provides a benefit for urban and vertiport use, where public acceptance depends on both emissions and acoustic footprint. This warrants the performance of a sustainability assessment at mission level. To this end, a dedicated *emissions tool* has been coupled to the Hybrid-Electric Mass and Range Solver: segment fuel flow and atmospheric state are taken from the mission calculation, direct CO_2 is estimated from fuel burn using the IPCC fuel-emission factor , and NO_x, CO, and HC are estimated with the Boeing Fuel Flow Method 2 (BFFM2), including altitude-dependent corrections to the emission indices . These species are then converted to CO_2-equivalent using the adopted aviation GWP factors .

At the 18% DoH design point, direct RMP CO_2 decreases from 1523 kg (3358 lb) for the baseline XV-15 to 1295 kg (2855 lb) for the HEXV-15, a reduction of approximately 15%. Total mission CO_2e decreases from approximately

1620 kg (3571 lb) to 1365 kg (3009 lb), corresponding to a reduction of about 16%. This percentage is slightly below the 18% energy-based DoH because electrical energy does not replace fuel burn one-to-one: hybridisation has caused an empty mass increase that must be compensated as well. CO_2 remains the dominant climate term, contributing approximately 94.88% of HEXV-15 CO_2e, while NO_x contributes approximately 5.04% despite its small emitted mass, which is because of its high GWP. The non-CO_2 contribution from NO_x, CO, and HC reduces from 97.4 kg (215 lb) to 69.9 kg (154 lb), a reduction of approximately 28%.

Noise is assessed for a 30 m (98 ft) observer below the aircraft in steady hover using the Lowson–Schlegel rotor-noise methodology as adapted by Made and Kurtz . This altitude is selected as it represents the start of the vertical descent phase for landings at vertiports . The method combines Lowson's rotational blade-passage formulation with Schlegel's broadband vortex-noise model . The resulting spectra are shown in Figure 18. The nominal HEXV-15 hover case is louder than the XV-15 because the Phase II aircraft operates at a higher VTOL mass and therefore requires higher rotor thrust: the overall tonal blade-passage level increases from 104.3 dB for the XV-15 to 106.3 dB for the nominal HEXV-15, while the overall vortex level increases from 91.0 dB to 92.2 dB.

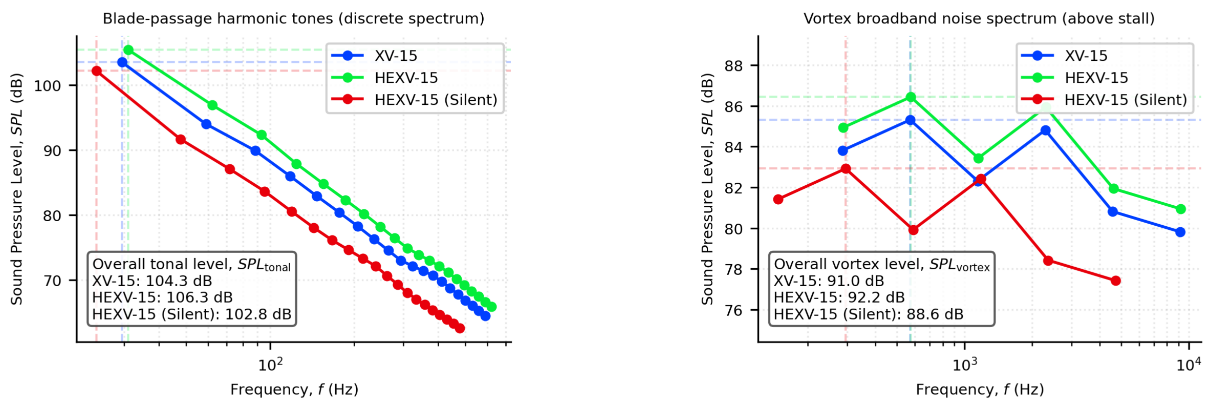

(a) Blade-passage tonal noise spectrum.

(b) Vortex broadband noise spectrum.

Figure 18: Hover noise spectra from the combined two proprotors at 30 m (98 ft) below the aircraft. The reduced-RPM silent mode reduces the tonal and broadband components relative to the nominal high-mass Kestrel hover case.

Simultaneously, *RPM scheduling* identifies the possibility of reduced-noise operating modes, one of which is shown in Figure 18. In this reduced-RPM "silent" mode, rotor speed is lowered and collective pitch is increased, reducing the overall blade-passage tonal level from 106.3 dB to 102.8 dB and the overall vortex level from 92.2 dB to 88.6 dB. The corresponding operating point stemmed from a high-level analysis in DUST, and remains compatible with the required hover thrust and shaft-power requirements. Electrification does not make RPM scheduling unique, but it makes the scheduling problem more flexible by adding controllable electrical torque support and reducing reliance on turboshaft transient response. The result is therefore not intended as an acoustic optimum, but as an indication that RPM, collective, and power-split scheduling can reduce vertiport and urban noise when used deliberately. If noise becomes a stronger operational driver, the rotor trade-off can shift additional weight toward noise reduction, since several retained candidates provided more favourable noise scores.

Cost, Maintainability, and Business-Case Consequences

Beyond reduced mission emissions, the relevance of the Kestrel is a financial result of its derivative-aircraft development logic. The HEXV-15 does not combine a clean-sheet vehicle with a novel hybrid-electric propulsion system; it retains the XV-15 tiltrotor layout, turboshaft backbone, and cross-shaft philosophy, while concentrating development effort on the hybrid-electric torque-assist system, modular batteries, wing extensions, and optimised proprotors. To quantify the commercial credibility of this strategy, a cost, maintainability, and business-case assessment was performed. The Non-Recurring Engineering (NRE) cost estimate is built up from engineering labour and tools, prototype manufacturing, tooling and set-up, and test/certification support, following conceptual aircraft cost-estimation logic and project-management cost decomposition .

Recurring unit cost is estimated bottom-up from composite structure production, rotor manufacture, COTS-based electric-chain procurement, retained T53-class propulsion hardware, secondary carry-over systems, final assembly, and QA/acceptance, with derivative-rotorcraft cost drivers and hybrid-electric integration risk used as bounding references . The mission-cost model then combines fuel, electricity, battery depreciation, maintenance, crew, and fees, using the RMP fuel burn, battery pack cost and life assumptions, fuel-price conversion, and a conservative rotorcraft maintenance reserve . The resulting quantities are summarised in Table 10.

Table 10: Economic and operational quantities used to assess the business case and commercial viability of the HEXV-15 Kestrel.

Metric	**Value**	**Interpretation**
NRE programme estimate	50.32 M EUR	Preliminary development, tooling, prototyping, testing, and certification allowance for a derivative programme.
Engineering cost	9.32 M EUR	Labour, programme overhead, software tools, office/workspace, and IT.
Prototype manufacturing	26.00 M EUR	Two flying prototypes and one static article, including hybrid-electric integration and test instrumentation.
Tooling and set-up	8.00 M EUR	Composite tooling, electrical-integration stations, assembly fixtures, and manufacturing preparation.
Testing and certification support	7.00 M EUR	Certification planning, compliance documentation, test support, and verification activities not already embedded in prototype manufacture.
LRIP recurring unit cost	7.0 M EUR	Low-rate aircraft cost estimate before production learning.
Learning-scaled unit cost	6.3 M EUR	Cost after 80% learning-curve scaling.
Hybrid-electric chain cost	0.236 M EUR	Motors, inverters, bus hardware, TMS, and 18% DoH modular battery set; modest relative to retained aircraft systems.
Implied sale price at 200 aircraft	7.7 M EUR	Includes NRE amortisation over 200 aircraft and an 18% margin.
Break-even production volume	36 aircraft	Approximate programme-level break-even point.
500 km (311 mi) mission cost	3176 EUR	Operating-cost estimate at 18% DoH.
Maintenance contribution	2400 EUR/mission	Dominant operating-cost term, approximately 75.6%.
Energy contribution	305 EUR/mission	Fuel plus electricity; approximately 10% of mission cost.
Technical / operational availability	91.7% / 71%	Six-year downtime model and 86 min mission plus 25 min turnaround.

The economic result shows that hybridisation does not make a tiltrotor commercially interesting through energy-price savings stemming from fuel savings: long-term maintenance (such as battery pack replacement) dominates the direct mission cost, whilst NRE amortisation logically dominates the programme case. The deliberate choice for a derivative architecture is therefore central to the business argument, because it limits clean-sheet certification exposure, preserves proven XV-15 heritage, and keeps the incremental hybrid-electric hardware cost small relative to the total aircraft. At the same time, the 36-aircraft break-even volume and 7.7 M EUR implied sale price indicate that the Kestrel can occupy a credible regional AAM position between short-range eVTOL aircraft and the much more expensive conventional tiltrotors. Future work should therefore prioritise maintainability, inspection burden, supplier-informed cost refinement, and certification evidence for the hybrid-electric chain, rather than treating further energy optimisation as the primary commercial lever.

Integrated preliminary-design conclusion

The HEXV-15 Kestrel demonstrates that hybridising a legacy tiltrotor is feasible only when the aircraft is redesigned around the mass and energy consequences of the hybrid system. The constrained Phase I study makes the failure mode explicit: batteries and electrical hardware consume the useful payload when they are imposed on the XV-15 under its original VTOL mass constraint. Phase II closes the aircraft by treating hybridisation as a system-level redesign problem. The final configuration carries 726 kg (1600 lb) of payload over the RMP at 18% energy-based DoH, with 415 kg (915 lb) of mission fuel and approximately 1303 kg (2873 lb) of installed battery mass.

The final design retains the aspects of the XV-15 that reduce programme risk: the tiltrotor layout, three-bladed proprotors, cross-shafted drivetrain philosophy, turboshaft energy backbone, and wing-borne cruise concept. Its originality is concentrated where it produces measurable aircraft-level benefit: nacelle-mounted wing extensions raise clean-wing L/D by 50%, proprotor optimisation raises installed hover FM by 16.0% and installed cruise propulsive efficiency by 6.7%, structural redesign recovers approximately 318 kg (701 lb) of primary structural mass, and modular batteries turn hybridisation into a dispatch variable rather than a permanent payload penalty. A system-level HEXV-15 Kestrel design parameter overview is shown in Table 11.

The value of the design does not lie in all questions being eliminated; it is that the right questions for further development have now become visible. Installed aerodynamics, aeroelasticity, conversion control, battery safety, thermal management, OEI/autorotation closure and further certification mapping are all necessary to formalise the design. The Phase II HEXV-15 Kestrel is thus a coherent derivative-aircraft answer to the RFP: optimised to reduce climate impact and to improve operating flexibility, but conceptually conservative enough to remain technically traceable, feasible, and realistic.

Integrated HEXV-15 Kestrel Design Result

The HEXV-15 Kestrel closes the Reference Mission Profile with 726 kg (1600 lb) payload and an 18% energy-based Degree of Hybridisation, while improving upon the legacy Bell XV-15 at aircraft level. This is attained through targeted optimisation and novel, derivative-aircraft design solutions: nacelle-mounted wing extensions, modular battery packaging, targeted proprotor improvements, and carbon/epoxy composite primary-structure designs with Omega-stiffened wingbox panels. The resulting Phase II vehicle reduces RMP fuel mass from 548 kg (1208 lb) to 415 kg (915 lb), reduces direct CO_2 from 1523 kg (3358 lb) to 1295 kg (2855 lb), improves HOGE ceiling from 2637 m (8652 ft) to 3014 m (9888 ft), reduces hover noise through clever employment of RPM scheduling, and pushes the maximum ferry range from 824 km (512 mi) to 1016 km (631 mi) at 17% energy DoH. With modular dispatch, the same aircraft allows for the operator to trade sustainability for range, resulting in configurations with up to a 58% energy DoH.

This is the direct result of treating hybridisation as a system-level optimisation problem that flows down into simultaneous subsystem design optimisation, rather than as a simple electrification exercise. In short: the HEXV-15 Kestrel is firmly established as a high-performance, near-term, certifiable, and affordable medium-range AAM tiltrotor concept.

Table 11: RFP design parameter overview of the HEXV-15 Kestrel.

Parameter	XV-15	Phase I	Phase II	Parameter	XV-15	Phase I	Phase II
Vehicle and Mission Sizing							
MTOM, VTOL, kg (lb)	5897 (13,000)	5897 (13,000)	6804 (15,000)	MTOM, STOL, kg (lb)	6804 (15,000)	6804 (15,000)	6804 (15,000)
Reported OEM, kg (lb)	4341 (9570)	4721 (10,408)	4360 (9612)	Payload VTOL, kg (lb)	755 (1665)	0 (0)	726 (1600)
Payload STOL, kg (lb)	Not Used in Development			Design fuel mass, kg (lb)	548 (1208)	488 (1076)	415 (915)
Geometry and Aerodynamic Performance							
Wing span, m (ft)	9.80 (32.2)	9.80 (32.2)	14.42 (47.3)	Wing area, m^2 (ft^2)	15.68 (169)	15.68 (169)	19.98 (215)
Wing extension length, m (ft)	–	–	2.31 (7.6)	Clean-wing L/D, –	23.40	23.40	35.10
Proprotor radius, m (ft)	3.81 (12.5)	3.81 (12.5)	3.74 (12.3)	Installed hover FM, –	0.603	0.603	0.718
Installed cruise η_{prop}, –	0.858	0.858	0.919	Hover rotor speed, RPM (rad/s)	586 (61.4)	586 (61.4)	621 (65.0)
Cruise rotor speed, RPM (rad/s)	518 (54.2)	518 (54.2)	312 (32.7)	HOGE ceiling, m (ft)	2637 (8652)	–	3014 (9888)
HIGE ceiling, m (ft)	3200 (10,499)	–	3568 (11,706)	Service ceiling, m (ft)	8800 (28,871)	–	9799 (32,149)
Propulsion and Hybrid-Electric Operation							
Peak VTOL MTOM Take-Off Power DoH, %	–	10	28	Cross-shaft redundancy?	Yes	Yes	Yes
Available power, turboshaft + electric, kW (hp)	2312 + 0 (3100 + 0)	2312 + 243 (3100 + 326)	2312 + 346.8 (3100 + 465)	Turboshaft engine mass, kg (lb)	667 (1470)	613 (1351)	667 (1470)
Energy-based DoH, design point, %	–	10	18	Design Depth of Discharge, %	–	90	71
Expected battery lifetime, years at two missions/day	–	Not Closed	4.08	Battery mass, kg (lb)	–	688 (1517)	1303 (2873)
Empty Mass Additions and Deletions							
Electric motor mass, kg (lb)	–	+74.1 (163)	+66.8 (147)	Electrical distribution mass, kg (lb)	–	+28.9 (64)	+48.2 (106)
Thermal management system mass, kg (lb)	–	+48.4 (107)	+43.8 (97)	Turboshaft downsizing, kg (lb)	–	-53.8 (-119)	Not Used
Wing structure, kg (lb)	–	–	-121.1 (-267)	Fuselage structure, kg (lb)	–	–	-170.1 (-375)
Empennage structure, kg (lb)	–	–	-24.6 (-54)	Rotor and cross-shaft, kg (lb)	–	–	-17.0 (-37)
Primary structure, kg (lb)	–	–	-318 (-701)	Hybrid-electric hardware excl. batteries, kg (lb)	–	+151.4 (334)	+158.8 (350)
System-Level Outcome							
Direct CO_2 on RMP, kg (lb)	1523 (3358)	–	1295 (2855)	Non-CO_2 CO_2e, kg (lb)	97.4 (215)	–	69.9 (154)
500 km (311 mi) mission cost, EUR	–	–	3176	NRE programme cost, M EUR	–	–	50.3
Recurring unit cost, LRIP / learning-scaled, M EUR	–	–	7.0 / 6.3	Technical / operational availability, %	–	–	91.7 / 71

HEXV-15 Three-View Drawing

ALL DIMENSIONS
IN MM AND INCH

TOP VIEW
(1:100)

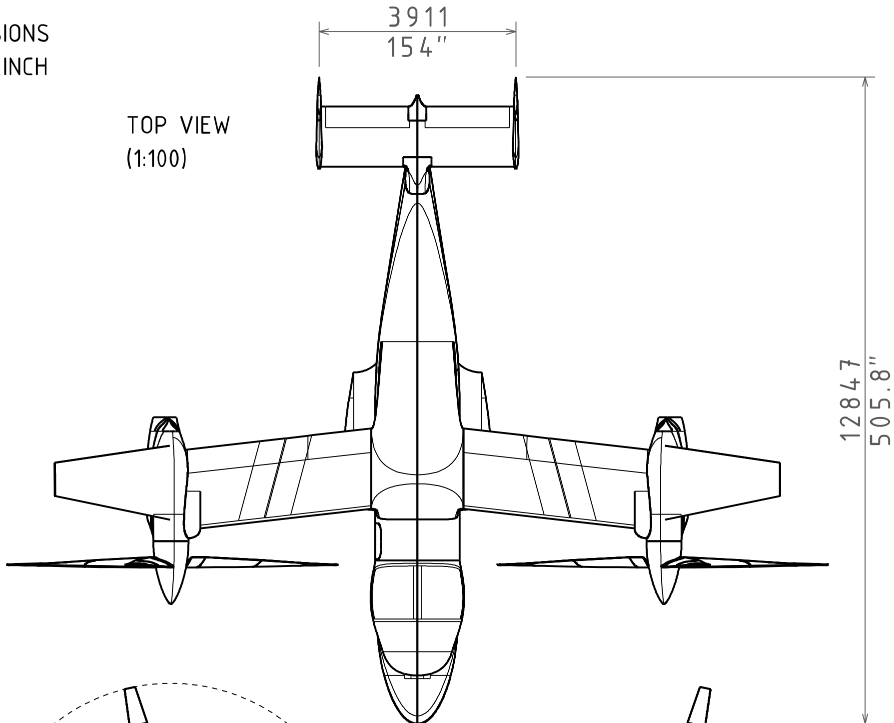

ISOMETRIC VIEW
(1:100)

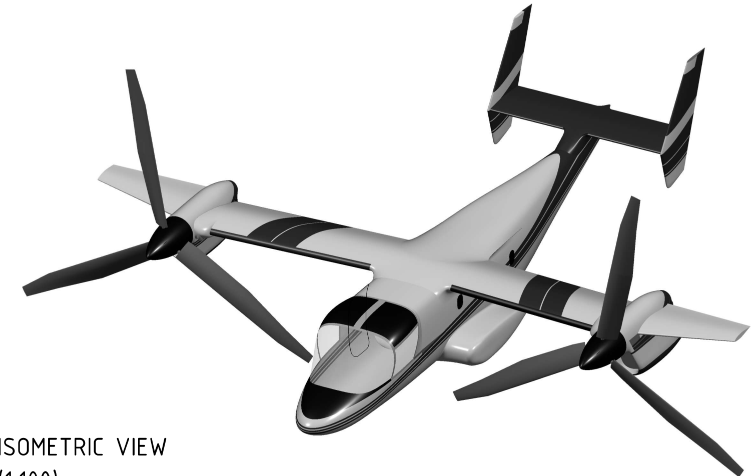

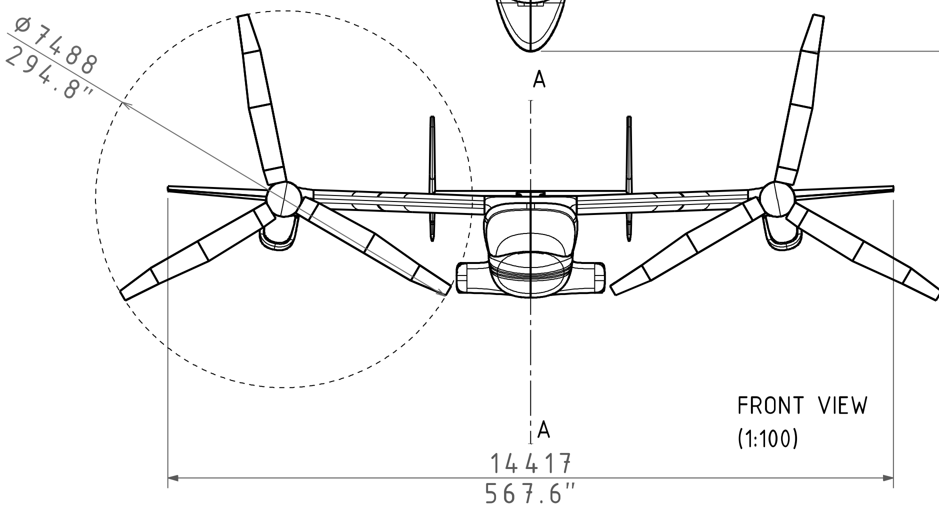

FRONT VIEW
(1:100)

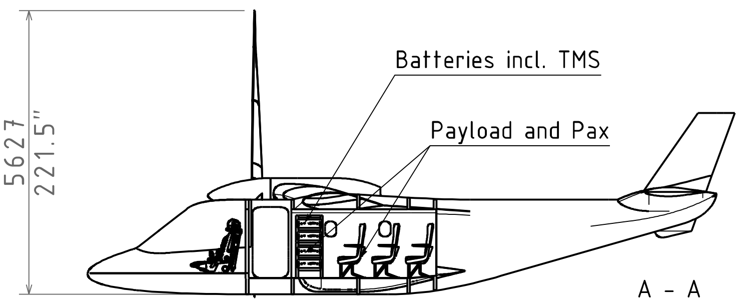

A - A
(1:100)

XX

		TUDelft		
		Description: Three-View Drawing and Isometric View of the Phase II HEXV-15 Kestrel Tiltrotor Design		
DRAWN BY Elias Gruters	DATE 30.05.2026			
CHECKED BY XXX	DATE XXX	SIZE ANSI A	Title HEXV-15 Kestrel	REV A1.1
DESIGNED BY XXX	DATE XXX	SCALE 1:100	WEIGHT (OEM): 4360kg (9612lbs)	SHEET 1/1